

The PAMELA experiment

P. Spillantini for the PAMELA collaboration

Abstract. The PAMELA equipment is in the assembling phase and in the next months will be installed on board of the Russian satellite Resurs DK; the launch is foreseen at the end of 2002. PAMELA is conceived to study the antiproton and positron fluxes in cosmic rays up to high energies: 190 GeV for \bar{p} and 270 GeV for e^+ . Other scientific purposes can be enumerated: search of antinuclei up to 30 GeV/n, with a sensitivity 10^{-7} in the \bar{He}/He ratio; determination of energy spectrum for nuclei with $Z \leq 6$ and for e^- ; measurement of the isotopic composition of light cosmic nuclei; monitoring of the cosmic ray flux at different phases of the solar cycle and study of the particles emitted in solar flares. During these years, from the first proposal of the experiment (1993) up to now, the configuration of the apparatus has been optimized doing simulations and tests, concerning both the physics and the technical characteristics. In this paper we report about the performances of all the detectors and the capability of the telescope in cosmic ray measurements.

1 Introduction

The PAMELA telescope (figure 1) will be launched in space in December 2002 and will enter a sun-synchronous orbit at $350 \div 600$ km of altitude and 70.4° of inclination. These orbital characteristics will allow a mission more than two year long and will enable the telescope to investigate the galactic component of cosmic rays close to poles, where the geomagnetic cut-off is lower.

PAMELA will detect antiprotons and positrons, allowing the measurement of the ratios \bar{p}/p and $e^+/(e^+ + e^-)$ with statistics never reached in balloon-borne experiments (see for instance (M. Boezio *et al.*, 2001) and references in) which are limited by the short duration of the mission and by the effects of the residual overlying atmosphere. In addition, these quantities will be measured in an energy range larger than that obtained in previous missions. The results of PAMELA will also complement data gathered by ground-based cosmic ray experiments.

The geometrical factor of the instrument is $20.5 \text{ cm}^2 \text{sr}$; as a consequence, during its mission PAMELA will detect more than $2 \times 10^4 \bar{p}$ and more than $2 \times 10^5 e^+$. The expected counting rate for the experiment is shown in figure 2 and it has been obtained taking into account the motion of the satellite along the orbit and the corresponding flux of cosmic and trapped particles in the PAMELA energy range ($E > 80$ MeV for protons and $E > 50$ MeV for electrons).

Correspondence to: P. Spillantini
(spillantini@fi.infn.it)

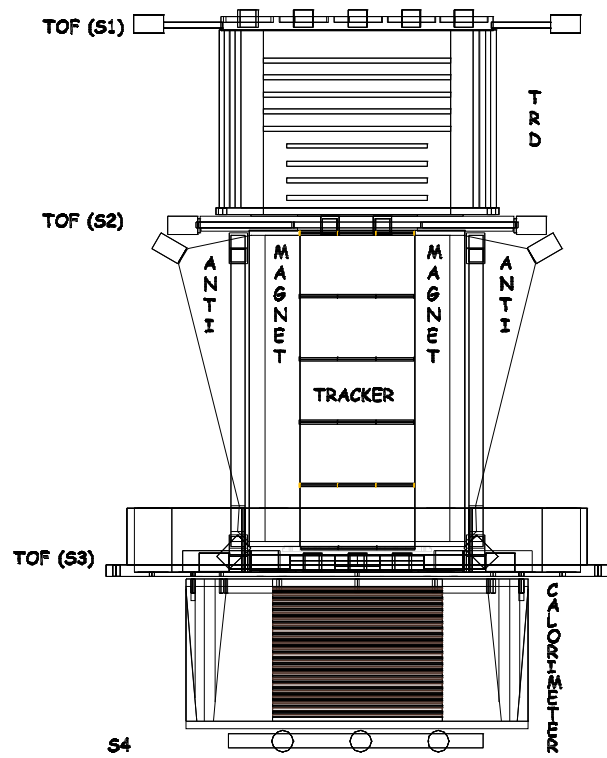


Fig. 1. The PAMELA telescope is about 1 m high and consists of a transition radiation detector, a magnetic spectrometer equipped with silicon microstrip detectors, a silicon/tungsten calorimeter, a time-of-flight detector, and an anti-coincidence system. The mass of the whole detector is about 400 kg.

2 Structure of the telescope

Magnetic spectrometer: it is composed by ferromagnetic modules, interleaved with six silicon microstrip detectors. The magnetic material is a Nd-Fe-B alloy, shaped in 5 blocks, each 80 mm high, with a rectangular cavity for the passage of cosmic rays, $132 \times 162 \text{ mm}^2$ wide. The intensity of the magnetic field is $\sim 0.48 \text{ T}$ at the center of the hole. The flight model of the magnet has been already built and a map of the field intensity has been done using a dedicated machine provided with a three axial probe.

The silicon planes cover the area of the cavity and are formed by a matrix of six double sided microstrip detectors, $70 \times 53 \text{ mm}^2$ and $300 \mu\text{m}$ thick, made of an *n*-type silicon wafer. Each plane is accommodated in a supporting structure, consisting of an aluminum frame 8 mm thick, designed to give the silicon sensor the needed mechanical resistance. The strip direction on the X view is suitable to detect the position of the

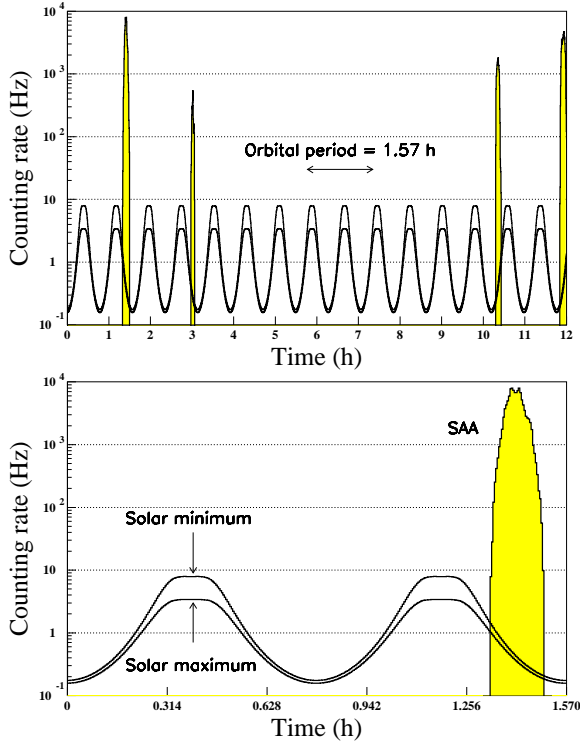


Fig. 2. The expected trigger rate of the experiment during a 12 hour period (above) and during an orbit (below). The passage in the South Atlantic Anomaly, where the flux of particles is several orders of magnitude larger, and the anticorrelation of the cosmic particles flux with the solar activity cycle are clearly visible.

track along the bending direction of charged particles; this view has p^+ -type strips with implantation pitch of $25 \mu\text{m}$ and read-out pitch of $50 \mu\text{m}$, without significantly degrading the spatial resolution: one can take advantage, in effect, from the capacitive coupling between two adjacent strips to collect the charge generated in the silicon wafer by the interacting particle. In the orthogonal direction, on the Y view, the n^+ -type strips are $67 \mu\text{m}$ apart. For this configuration there are 36864 electronics channels in the tracker.

The spatial resolution reachable utilizing this geometry is $3.0 \pm 0.1 \mu\text{m}$ on the junction side (fig. 3) and $11.5 \pm 0.6 \mu\text{m}$ on the ohmic side. The non-gaussian tail in figure 3 is associated with high multiplicity events and could be explained with emission of δ -rays in the silicon layer. The signal-to-noise ratio (for Minimum Ionizing Particles) for these detectors is about 50 for the X view and 25 for the Y view, ensuring high efficiency in cluster recognition.

The Maximum Detectable Rigidity (MDR) of this spectrometer is $800 \text{ GV}/c$, but the proton and electron spillover background sets a limit value for the energy of $\sim 200 \text{ GeV}$ for \bar{p} and $\sim 300 \text{ GeV}$ for e^+ .

Calorimeter: the electromagnetic sampling calorimeter utilizes single-sided silicon planes (segmented in macrostrips, with pitch 2.4 mm) and tungsten layers as absorber. The

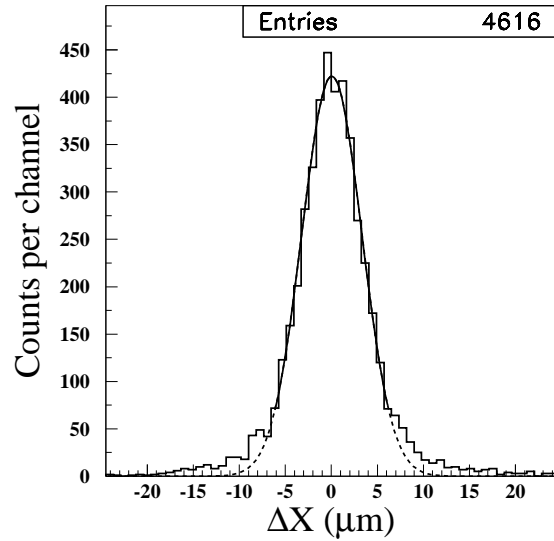


Fig. 3. Measured spatial resolution on the junction side of the silicon planes (X view), where the read-out pitch is $50 \mu\text{m}$.

calorimeter of PAMELA is composed by 11 modules, each formed by two series of: silicon plane (X view), absorber (2.3 mm thick), silicon plane (Y view) for a total number of 44 silicon layers $380 \mu\text{m}$ thick and 22 absorber layers. The total thickness of the calorimeter corresponds to 0.9 interaction lengths and 16 radiation lengths. Each plane is $240 \times 240 \text{ mm}^2$ wide and is an array of nine basic detecting units. This kind of calorimeters has been already utilized by the WiZard collaboration in several balloon-borne experiments, obtaining high reliability and good performances (The WiZard collaboration (1993); M. Ricci *et al.* (1999)).

The calorimeter of PAMELA, endowed with high granularity, can reconstruct the particle path inside the detector volume and measure the energy deposit of the complete electromagnetic shower, providing separation between leptons and hadrons at high confidence level. The rejection power of the calorimeter has been measured in a test beam session at SPS, in July 2000. Here the separation between electrons and pions at momentum $100 \text{ GeV}/c$ has been studied using a reduced number of modules in the calorimeter with respect to the final configuration. Extrapolating these results for the flight model one expects an energy resolution $< 5\%$ between 20 and 100 GeV and a rejection power of 10^4 for protons and electrons in antiproton and positron measurements (selection efficiency 95%). In figure 4 the total number of hit strips as a function of the total energy release is reported for a sample of SPS events and the good separation between leptons and hadrons can be observed.

Transition Radiation Detector: this is a threshold detector which utilizes the X-radiation emitted by high energy particles crossing the interface between media with different dielectric constants. The PAMELA TRD can identify

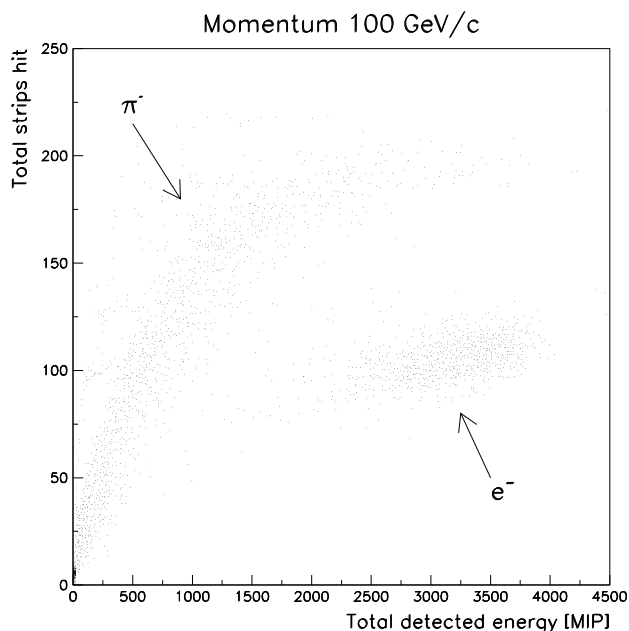


Fig. 4. The separation capability between e^- and π^- for the calorimeter prototype at a given value of the momentum (100 GeV/c). The total number of hit strips as a function of the energy deposit is reported.

leptons out of hadrons up to several hundred GeV detecting the radiation produced when a cosmic particle passes through 10 planes of carbon fibre radiator. This radiation is detected by straw tubes planes, interleaved with the radiators. A total of 1024 tubes, 280 mm long and 4 mm in diameter, are used; they work in proportional regime, maximizing the photon conversion capability, thanks to both the gas mixture used (80% Xe and 20% CO₂) and the operating high voltage: 1400 V (the gas is furnished by an on-board storage of 1.50 m³, at STP). The straw signal is acquired using a pulse-height measurement technique. The π^- -contamination of 5% at 90% of electron selection efficiency, is in good agreement with the actual one estimated from beam tests (figure 5). In the plot one can see that radiating particles, like electrons, release a greater amount of energy, due to transition radiation, with respect to pions, whose energy loss follows a Landau distribution (see also the PAMELA TRD contribution in this conference).

Time Of Flight system : in the framework of the experiment it has three primary tasks. The TOF in fact provides the trigger to the other detectors and to the data acquisition, selects albedo particles with very high accuracy (by means of the determination of the sign of β) and reduces the particle contamination in antiparticle measurement below ~ 1 GeV. It is composed by five planes of scintillation counters 7 mm thick, two on the top of the telescope, one upon the magnet and the last two below the tracking system. Each plane is divided in narrow, long sectors, which are read by two photomultipliers at the opposite ends. These sectors are disposed mutually orthogonal in adjacent planes, so to provide a rough

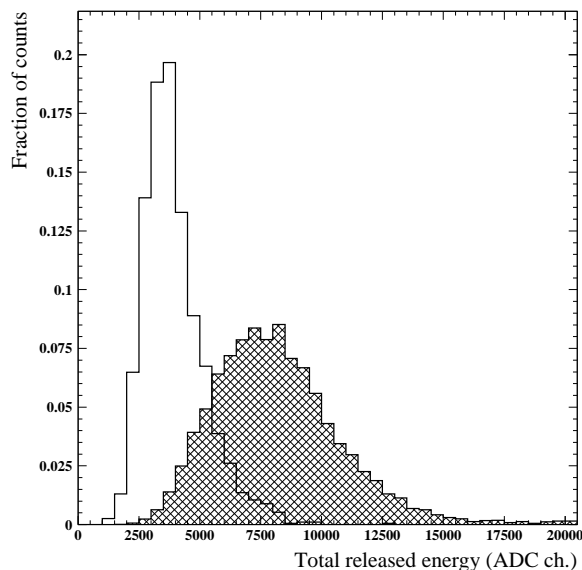


Fig. 5. Fraction of counts for electrons (shaded region) and pions as a function of the energy release in the TRD. This plot has been obtained with data gathered at SPS in July 2000 where e^- and π^- at momentum 40 GeV/c were utilized.

estimate of the particle impact point. The time resolution of each sector is about 120 ps. All the TOF planes cover an area corresponding to the angular aperture of the telescope, so to optimize the trigger and the rejection of upward moving particles.

AntiCoincidence system : in PAMELA two different AC detectors are present and they cover all the solid angle excluded by the angular aperture of the telescope, upon and around the magnet. These detectors consist of scintillator planes 8 mm thick, read-out by photomultipliers similar to those present in the TOF system. The anticounter front-end electronics sends discriminated PMT pulse information to the anticounter data acquisition board which in turn is connected to the global data acquisition system.

3 Conclusions

At the present the PAMELA project is completely defined and the flight model is under construction. All the tests confirm that the scientific requirements are reachable and that PAMELA can significantly contribute to the knowledge of antiparticle and particle spectra in cosmic rays. Up to now with balloon flights only ~ 500 antiprotons have been detected (figure 6); the PAMELA apparatus will be capable in the next years to collect more than $2 \times 10^4 \bar{p}$ and $2 \times 10^5 e^+$ giving us high-statistic information on the behavior of the spectrum above 40 GeV (where no measurements are available). In this way theoretical models can be tested, understanding if the antiproton flux is consistent with secondary production in the interstellar medium or if primary sources

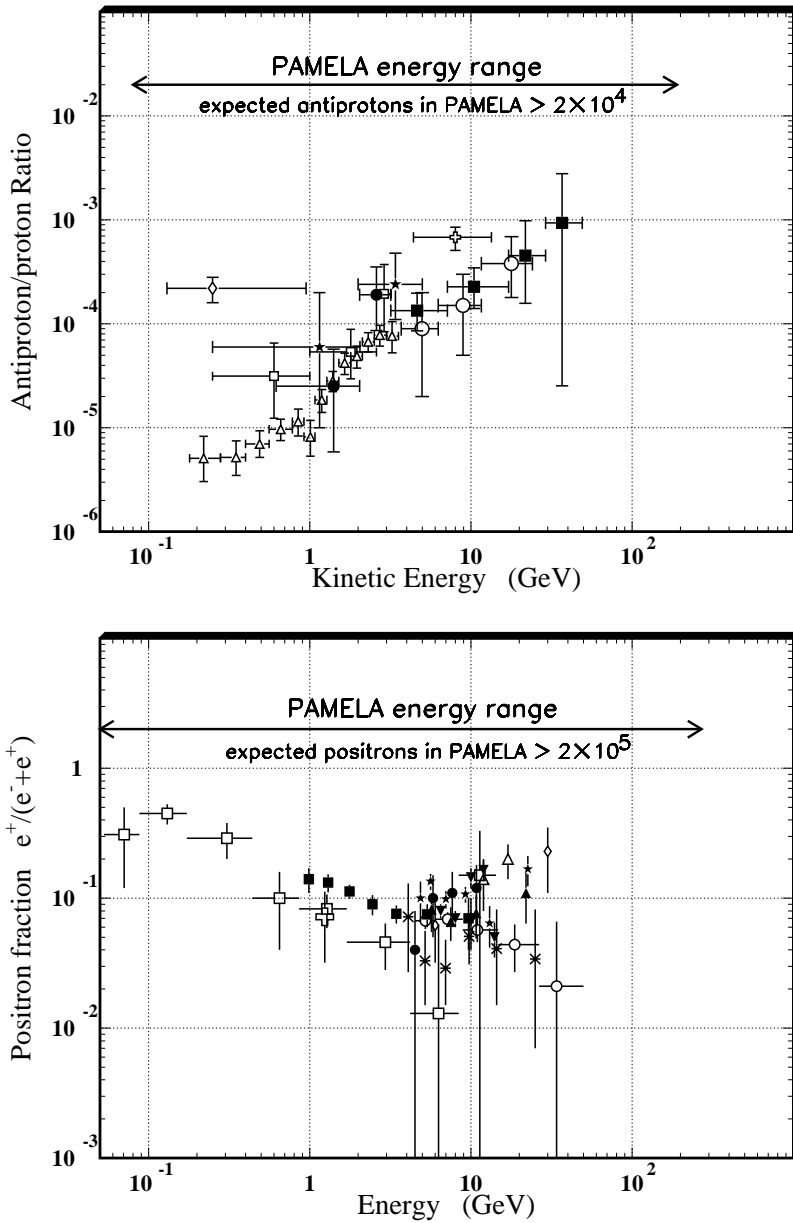


Fig. 6. In this figure the ratios \bar{p}/p (above) and $e^+/(e^+ + e^-)$ (below) are reported, obtained with balloon-borne missions. Up to now, in balloon flights, only about 500 \bar{p} have been detected and about 10 for $E > 10$ GeV. PAMELA can provide high statistics measurements of this quantities, spanning over three decades in energy with the same detector. In addition the residual atmospheric depth for PAMELA will be negligible, compared with that present at altitudes reachable with balloons. A monitoring of \bar{p} and e^+ fluxes at different periods of the solar cycle can also be done for low-energy particles and antiparticles.

Measurements for antiprotons: (■ M. Boezio *et al.* (2001); ● M. Boezio *et al.* (1997); ○ G. Basini *et al.* (1999); △ S. Orito *et al.* (2000); □ J. Mitchell *et al.* (1996); ◇ A. Buffington *et al.* (1981); ★ E. A. Bogomolov (1987) and E. A. Bogomolov (1990); ✱ R.L. Golden (1984)).

Measurements for positrons: (* M. Boezio *et al.* (1999); ▼ G. Basini *et al.* (1995); ▲ R.L. Golden *et al.* (1996); ■ M. Boezio *et al.* (2000); ● R.L. Golden *et al.* (1994); ○ S.W. Barwick (1997); ★ R.L. Golden *et al.* (1987); △ D. Müller *et al.* (1987); □ J. Faselow *et al.* (1969); ◇ A. Buffington *et al.* (1975); ✱ J.M. Clem *et al.* (1996)).

must be introduced to explain the observed spectrum.

References

- S.W. Barwick *et al.* 1997, ApJ 482,L191
 G. Basini *et al.* 1995, Proc. 24th ICRC (Rome), OG.7.1.1
 G. Basini *et al.* 1999, Proc. 26th ICRC (Salt Lake City), OG.1.1.21
 M. Boezio *et al.* 1997, ApJ 487,415
 M. Boezio *et al.* 1999, Proc. 26th ICRC (Salt Lake City), OG.1.1.16
 M. Boezio *et al.* 2000, ApJ 532,653
 M. Boezio *et al.* 2001, preprint astro-ph 0103513, submitted to ApJ.
 E. A. Bogomolov 1987, Proc. 20th ICRC (Moscow) 2,72
 E. A. Bogomolov 1990, Proc. 21th ICRC (Adelaide) 3,288
 A. Buffington *et al.* 1975, ApJ 199,699
 A. Buffington *et al.* 1981, ApJ 248,1179
 J.M. Clem *et al.* 1996, ApJ 464,507
 J. Faselow *et al.* 1969, ApJ 158,771
 R.L. Golden 1987, A&A 188,145
 R.L. Golden 1984, Astrophys. Lett. 24,75
 R.L. Golden *et al.* 1994, ApJ 436,769
 R.L. Golden *et al.* 1996, ApJ 457,L103
 J. Mitchell *et al.* 1996, Phys. Rev. Lett. 76,3057
 D. Müller *et al.* 1987, Proc. 21th ICRC (Adelaide) 3,249
 S. Orito *et al.* 2000, Phys. Rev. Lett. 84,1078
 M. Ricci *et al.* 1999, Proc. 26th ICRC (Salt Lake City), OG.4.1.13
 The PAMELA collaboration 1995, Proc. 24th ICRC (Rome), OG 10.3.7
 The PAMELA collaboration 1997, Proc. 25th ICRC (Durban), OG.10.2.9
 The PAMELA collaboration 1999, Proc. 26th ICRC (Salt Lake City), OG.4.2.04
 The WIZARD collaboration 1993, Nuclear Physics B 32,77.